Machine Learning Forecasting and GAN-Based Scenario Control for EV Charging and PV Integration

Fatemeh Nasr Esfahani

School of Engineering

Lancaster University

Lancaster, UK

f.nasresfahani@lancaster.ac.uk

Neeraj Suri
School of Computing and Communications
Lancaster University
Lancaster, UK
neeraj.suri@lancaster.ac.uk

Xiandong Ma
School of Engineering
Lancaster University
Lancaster, UK
xiandong.ma@lancaster.ac.uk

Abstract—The increasing integration of electric vehicles (EVs) and photovoltaic (PV) generation introduces significant uncertainty into modern distribution grids. This paper presents a dualstage, AI-driven framework for resilient energy management that combines machine learning-based forecasting with generative modelling for scenario-based control. The first stage uses a hybrid forecasting architecture: long short-term memory (LSTM) and convolutional LSTM (ConvLSTM) models for EV demand prediction and eXtreme gradient boosting (XGBoost) for PV generation forecasting. The second stage employs a generative adversarial network (GAN) to produce realistic EV and PV scenarios, capturing both typical variability and a wide range of operating conditions. The framework is validated on a modified IEEE 33-bus distribution system with integrated EV charging and stationary storage. Results show that the dual-model forecasting approach achieves high accuracy across diverse temporal patterns, while GAN-based scenario generation improves the adaptability of control decisions. Scenario-based optimisation enhances performance under uncertainty, especially at highvariance nodes, and offers greater flexibility than deterministic control in balancing energy cost and demand satisfaction.

Index Terms—Electric vehicles, Photovoltaic, Machine learning, Generative adversarial networks, Forecasting, Optimisation

I. INTRODUCTION

Electric vehicles (EVs) offer a promising pathway to decarbonise transportation, while photovoltaic (PV) systems represent a clean, renewable source of energy [1]–[3]. However, their increasing presence introduces significant operational challenges to power systems due to the stochastic and often uncoordinated nature of their energy profiles. EV charging is influenced by highly variable user behaviour, including unpredictable arrival and departure times as well as clustering in charging demand [4]. Similarly, PV generation depends heavily on environmental conditions such as solar irradiance, which are inherently uncertain and variable [5].

Traditional power systems, designed for centralised, predictable loads, are ill-equipped to manage the dynamic, distributed, and inverter-based nature of modern resources like EVs and PVs [6]. This shift underscores the need for advanced forecasting and control strategies to maintain grid reliability amid high penetrations of such uncertain and variable technologies.

Data-driven methods have become prominent for short-term forecasting due to their adaptability and ability to capture complex nonlinear patterns. For PV generation, models such as gradient boosting (GB), support vector machines (SVM), and deep neural networks, including long short-term memory (LSTM), are widely used [5]. Forecasting EV charging demand is more challenging due to behavioural and spatiotemporal variability. Deep learning models like LSTM, convolutional LSTM (ConvLSTM), and bidirectional ConvLSTM (BiConvLSTM) have proven effective for modelling these dependencies [4]. Hybrid frameworks that combine machine learning with heuristic optimisation have also been proposed to enhance prediction accuracy and inform charging station siting and resource planning [7], [8]. However, most existing forecasting approaches treat EV and PV systems in isolation, ignoring their interactive effects on grid dynamics. Conventional model-based methods also struggle to represent the complex nonlinear and spatial interactions introduced by these distributed resources.

Beyond point forecasts, there is a growing need to anticipate rare or adversarial events, such as atypical weather conditions or abrupt demand spikes, that are poorly represented in historical data. Generative adversarial networks (GANs) have emerged as a powerful tool for uncertainty-aware modelling [9]. By learning underlying data distributions, GANs can generate diverse and realistic synthetic scenarios that enhance decision-making under uncertainty. Recent applications include coordinated management of PV-integrated EV parking lots [10], explainable EV energy profiling using ensemble learning [11], and uncertainty-aware microgrid scheduling [12]. However, many existing GAN-based approaches model EV and PV behaviours independently and often struggle to preserve temporal realism, particularly under edge case conditions, leading to scenarios that may compromise control performance.

Building on these developments, this paper introduces a dual-stage, AI-driven framework that integrates short-term forecasting with uncertainty-aware control. The first stage employs LSTM and ConvLSTM models for forecasting EV

charging demand and eXtreme gradient boosting (XGBoost) for PV generation prediction. The second stage uses GANs to generate realistic and diverse scenarios, including rare and adversarial events, which are then incorporated into a scenario-based control strategy for resilient energy management.

The remainder of the paper is structured as follows: Section II details the machine learning models used for forecasting EV charging and PV generation. Section III presents the GAN-based scenario generation and the control optimisation strategy. Section IV describes the case study setup and evaluates the forecasting accuracy, scenario realism, and control performance. Finally, Section V concludes the paper.

II. FORECASTING WITH MACHINE LEARNING

Forecasting models for EV charging and PV generation are constructed using historical and contextual features. Let \mathcal{B} denote the set of buses in the distribution network. The forecasting task is to learn two distinct mapping functions:

$$\begin{cases} \hat{P}_{\text{EV},b}(t+\tau) = \mathcal{F}_{\text{EV}}\left(\mathbf{x}_{b}^{\text{EV}}(t), \dots, \mathbf{x}_{b}^{\text{EV}}(t-\Delta+1)\right) \\ \hat{P}_{\text{PV},b}(t+\tau) = \mathcal{F}_{\text{PV}}\left(\mathbf{x}_{b}^{\text{PV}}(t), \dots, \mathbf{x}_{b}^{\text{PV}}(t-\Delta+1)\right) \end{cases}, \quad b \in \mathcal{B} \quad (1)$$

where $P_{\mathrm{EV},b}(t)$ and $P_{\mathrm{PV},b}(t)$ represent the actual EV charging and PV generation power (in kW) at bus b and time t, and $\hat{P}_{\mathrm{EV},b}(t+\tau)$, $\hat{P}_{\mathrm{PV},b}(t+\tau)$ are their predicted values at horizon τ , while $\mathcal{F}_{\mathrm{EV}}$ and $\mathcal{F}_{\mathrm{PV}}$ denote the respective forecasting models (e.g., LSTM/ConvLSTM and XGBoost), applied to input feature sequences of length Δ . Here, $t \in \mathbb{Z}$ denotes discrete time steps (e.g., hourly intervals), and $\tau \in \{1,2,\ldots,H\}$ is the forecast horizon in discrete units. Each input vector $\mathbf{x}_b^{(\cdot)}(t) \in \mathbb{R}^n$ represents recent history, temporal features (e.g., hour of day, day of week), and exogenous variables (e.g., temperature, irradiance). The model uses a lookback window of length Δ to forecast over a horizon $H \ll T$, where $\mathcal{T} = \{1,2,\ldots,T\}$ represents the total time horizon. This corresponds to a lookback window spanning from $t-\Delta+1$ to t, comprising exactly Δ discrete time steps.

A. EV/ESS load forecasting

To forecast EV and ESS load, an LSTM-based recurrent neural network is employed, well-suited for modelling time series with long-range dependencies due to its internal gating mechanisms that regulate information flow across time steps.

The training dataset is constructed by applying a sliding window of length Δ over $\mathcal{T}^{\text{EV}}_{\text{train}} \subseteq \mathcal{T}$, extracting overlapping input-output pairs. For each EV-enabled bus $b \in \mathcal{B}_{\text{EV}} \subseteq \mathcal{B}$, this results in $T - \Delta - H + 1$ training samples. Each sample consists of an input sequence of contextual features over the past Δ time steps and a target sequence of future EV charging power over the forecast horizon H. These samples are aggregated across all relevant buses to form the complete training set.

Let the input sequence for bus b at time t be defined as:

$$\mathbf{X}_{b}^{\text{EV}}(t) = [\mathbf{x}_{b}^{\text{EV}}(t - \Delta + 1), \dots, \mathbf{x}_{b}^{\text{EV}}(t)] \in \mathbb{R}^{\Delta \times n}, \tag{2}$$

where each feature vector encodes the observed EV charging power and associated contextual variables at time t as below:

$$\mathbf{x}_b^{\text{EV}}(t) = \left[P_{\text{EV},b}(t), \ \mathbf{t}^{\text{EV}}(t), \ \mathbf{w}(t), \ \mathbf{e}(t) \right], \tag{3}$$

with $\mathbf{t}^{\mathrm{EV}}(t) \in \mathbb{R}^{n_t}$ being temporal features (e.g., hour of day, weekday), $\mathbf{w}(t) \in \mathbb{R}^{n_w}$ containing weather variables, and $\mathbf{e}(t) \in \mathbb{R}^{n_e}$ capturing event-based indicators. The full input dimensionality is $n = 1 + n_t + n_w + n_e$.

The model learns a function to map these sequences to future EV charging forecasts $\hat{\mathbf{P}}_{\text{EV},b}(t+1:t+H) = \text{LSTM}_{\theta_{\text{EV}}}(\mathbf{X}_b^{\text{EV}}(t))$, where $\hat{\mathbf{P}}_{\text{EV},b} \in \mathbb{R}^H$ is the predicted EV power profile over H future time steps and θ_{EV} represents the complete set of learnable parameters (e.g., recurrent weights, biases, and output layer parameters). The LSTM update at each time step t is given by $(\mathbf{h}_t, \mathbf{c}_t) = \text{LSTMCell}(\mathbf{x}_t, \mathbf{h}_{t-1}, \mathbf{c}_{t-1})$, where the gating operations are:

$$\begin{cases} \psi_t^{(g)} = \sigma(\mathbf{W}_g \mathbf{x}_t + \mathbf{U}_g \mathbf{h}_{t-1} + \mathbf{b}_g), & g \in \{f, i, o\} \\ \tilde{\mathbf{c}}_t = \tanh(\mathbf{W}_c \mathbf{x}_t + \mathbf{U}_c \mathbf{h}_{t-1} + \mathbf{b}_c) \\ \mathbf{c}_t = \mathbf{f}_t \odot \mathbf{c}_{t-1} + \mathbf{i}_t \odot \tilde{\mathbf{c}}_t \\ \mathbf{h}_t = \mathbf{o}_t \odot \tanh(\mathbf{c}_t) \end{cases}$$
(4)

where $g \in \{f, i, o\}$ denotes the forget, input, and output gates, σ is the sigmoid function, \odot denotes element-wise multiplication, and $\{\mathbf{W}, \mathbf{U}, \mathbf{b}\}$ are learnable weights and biases.

When multiple EV charging stations (EVCSs) at different buses exhibit spatial dependencies, a ConvLSTM is used. The input becomes a 3D tensor $\mathbf{X}(t) \in \mathbb{R}^{\Delta \times H \times W}$, where $H \times W$ encodes the spatial layout. The cell operations now use convolution [4]:

$$\begin{cases}
\mathbf{\Psi}_{t}^{(g)} = \sigma(\mathbf{W}_{g} * \mathbf{X}_{t} + \mathbf{U}_{g} * \mathbf{H}_{t-1} + \mathbf{b}_{g}), & g \in \{f, i, o\} \\
\tilde{\mathbf{C}}_{t} = \tanh(\mathbf{W}_{c} * \mathbf{X}_{t} + \mathbf{U}_{c} * \mathbf{H}_{t-1} + \mathbf{b}_{c}) \\
\mathbf{C}_{t} = \mathbf{f}_{t} \odot \mathbf{C}_{t-1} + \mathbf{i}_{t} \odot \tilde{\mathbf{C}}_{t} \\
\mathbf{H}_{t} = \mathbf{o}_{t} \odot \tanh(\mathbf{C}_{t})
\end{cases}$$
(5)

where * denotes the convolution operator.

The model is trained to minimise a composite loss function that combines mean absolute error (MAE) and mean squared error (MSE) across all buses and forecast steps as below:

$$\mathcal{L}(P_{\text{EV}}, \hat{P}_{\text{EV}}) = \frac{1}{|\mathcal{B}|H} \sum_{b \in \mathcal{B}} \sum_{\tau=1}^{H} \left[\alpha_1 \cdot \left| P_{\text{EV},b}(t+\tau) - \hat{P}_{\text{EV},b}(t+\tau) \right| + \alpha_2 \cdot \left(P_{\text{EV},b}(t+\tau) - \hat{P}_{\text{EV},b}(t+\tau) \right)^2 \right]$$
(6)

where α_1 and α_2 are non-negative weighting coefficients.

Algorithm 1 outlines the training process, which proceeds over multiple epochs. In the LSTM model, the final hidden state \mathbf{h}_{Δ} is passed through a fully connected layer to produce the forecast. In ConvLSTM, the spatiotemporal hidden state \mathbf{H}_{Δ} is decoded via a convolutional output layer, preserving spatial relationships across EVCS nodes (buses). Model parameters θ_{EV} are updated via gradient descent using the $\theta_{\mathrm{EV}} \leftarrow \theta_{\mathrm{EV}} - \ell_{\mathrm{EV}} \cdot \nabla_{\theta_{\mathrm{EV}}} \mathcal{L}$ to minimise the loss in Eq. (6), with learning rate ℓ_{EV} . After each epoch, validation loss $\mathcal{L}_{\mathrm{val}}$ is computed for model selection and early stopping. The final trained model, $\mathrm{LSTM}_{\theta_{\mathrm{EV}}}$ or $\mathrm{ConvLSTM}_{\theta_{\mathrm{EV}}}$, maps historical inputs to forecasts $\hat{\mathbf{P}}_{\mathrm{EV},b}(t+1:t+H) \in \mathbb{R}^H$ for each EVenabled bus $b \in \mathcal{B}_{\mathrm{EV}}$.

B. PV generation forecasting

XGBoost is employed for PV generation forecasting due to its efficiency and accuracy on structured data. Its suitability

Algorithm 1 EV/ESS load forecasting using LSTM or ConvLSTM

```
1: Input: Training data \{\mathbf{X}(t), P_{\mathrm{EV}}(t)\}_{t=1}^T, validation set, window size \Delta, forecast horizon H, learning rate \ell_{\mathrm{EV}}, max epochs E
      Initialise: Model parameters \theta_{\rm EV}, best validation loss \mathcal{L}_{\rm best} \leftarrow \infty
      for epoch e = 1 to E do
             for each time step t \in [\Delta, T - H], where T = |\mathcal{T}| do
                   if LSTM then
 6:
                         Extract input window \mathbf{X}_{t-\Delta+1:t} \in \mathbb{R}^{\Delta \times n}
 7:
8:
                         Initialise hidden states \mathbf{h}_0, \mathbf{c}_0 \leftarrow \mathbf{0}
                   else if ConvLSTM then
                         Extract input tensor \mathbf{X}_{t-\Delta+1:t} \in \mathbb{R}^{\Delta \times H \times W} Initialise hidden states \mathbf{H}_0, \mathbf{C}_0 \leftarrow \mathbf{0}
10:
11:
12:
                    for each time index k=1 to \Delta do
13:
                          if LSTM then
                                Compute gates \psi_k^{(g)}, \tilde{\mathbf{c}}_k using Eq. (4) Update states \mathbf{c}_k, \mathbf{h}_k using Eq. (4)
14:
15:
                          else if ConvLSTM then Compute gates \Psi_k^{(g)}, \check{\mathbf{C}}_k using Eq. (5) Update states \mathbf{C}_k, \mathbf{H}_k using Eq. (5)
16:
17:
18:
19:
                          end if
                    end for
20:
21:
                    Generate forecast:
                 LSTM: \hat{\mathbf{P}}_{EV}(t+1:t+H) = MLP(\mathbf{h}_{\Delta})
                 ConvLSTM: \hat{\mathbf{P}}_{\text{EV}}(t+1:t+H) = \text{ConvOutput}(\mathbf{H}_{\Delta})
22:
                    Compute training loss \mathcal{L}(P_{\text{EV}}, \hat{P}_{\text{EV}}) using Eq. (6)
23:
                    Update model: \theta_{\text{EV}} \leftarrow \theta_{\text{EV}} - \ell_{\text{EV}} \cdot \nabla_{\theta_{\text{EV}}} \mathcal{L}(P_{\text{EV}}, \hat{P}_{\text{EV}})
24:
25:
              end for
              Evaluate model on validation set:
26:
27:
28:
29:
                      \mathcal{L}_{val} \leftarrow ValidationLoss(\theta_{EV})
              if \mathcal{L}_{val} < \mathcal{L}_{best} then
                    Save current model; \mathcal{L}_{best} \leftarrow \mathcal{L}_{val}
              end if
30:
              if early stopping condition met then
31:
                   break
32:
              end if
33: end for
34: Output: Trained model LSTM_{\theta_{EV}} or ConvLSTM_{\theta_{EV}}, mapping input \mathbf{X}_b^{EV}(t) to
       forecast \hat{\mathbf{P}}_{\text{EV},b}(t+1:t+H)
```

for short-term prediction stems from its ability to capture nonlinear relationships in environmental and temporal features such as irradiance, temperature, and time-of-day.

The training dataset for each PV-enabled bus $b \in \mathcal{B}_{PV} \subseteq \mathcal{B}$ is constructed as a set of independent samples:

$$\mathbf{X}_{b}^{\mathrm{PV}} = \left\{ \left(\mathbf{x}_{b}^{\mathrm{PV}}(t), P_{\mathrm{PV}, b}(t+\tau) \right) \right\}_{t \in \mathcal{T}_{\mathrm{rein}}^{\mathrm{PV}}} \tag{7}$$

where $\mathbf{x}_b^{\mathrm{PV}}(t) \in \mathbb{R}^n$ is the input feature vector at time t, and $P_{\mathrm{PV},b}(t+\tau)$ is the target PV output at the desired forecast horizon τ . Each input vector $\mathbf{x}_b^{\mathrm{PV}}(t)$ consists of:

$$\mathbf{x}_{b}^{\text{PV}}(t) = \left[f_{\text{irr}}(t), \ T_{\text{amb}}(t), \ \mathbf{t}^{\text{PV}}(t) \right], \tag{8}$$

where $f_{\rm irr}(t)$ is the solar irradiance (kW/m²), $T_{\rm amb}(t)$ is the ambient temperature (°C), and ${\bf t}^{\rm PV}(t) \in \mathbb{R}^{n_t}$ encodes temporal attributes (e.g., hour of day, day of year, seasonality). The model learns a mapping function $\hat{P}_{\rm PV}, b(t+\tau) = {\rm XGBoost}_{\theta_{\rm PV}}({\bf x}_b^{\rm PV}(t))$, where $\theta_{\rm PV}$ denotes the set of learned parameters across the ensemble of decision trees.

The XGBoost model is trained to minimise the MAE over the training samples, along with a regularisation term $\Omega(\theta_{PV})$ that penalises model complexity (e.g., number of leaves, tree depth):

$$\mathcal{L}(P_{\text{PV}}, \hat{P}_{\text{PV}}) = \frac{1}{|\mathcal{M}|} \sum_{(t,b) \in \mathcal{M}} \left| P_{\text{PV},b}(t+\tau) - \hat{P}_{\text{PV},b}(t+\tau) \right| + \Omega(\theta_{\text{PV}}),$$

The loss is evaluated over samples $(t,b) \in \mathcal{M}$, with $\mathcal{M} \subseteq \mathcal{T}^{PV}_{train} \times \mathcal{B}_{PV}$.

Algorithm 2 PV generation forecasting using XGBoost

```
1: Input: Training data \left\{\left(\mathbf{x}_b^{\mathrm{PV}}(t), P_{\mathrm{PV},b}(t+\tau)\right)\right\}_{t\in\mathcal{T}_{\mathrm{train}}^{\mathrm{PV}},\ b\in\mathcal{B}_{\mathrm{PV}}}; validation set; learning rate \ell_{\mathrm{PV}}; max boosting rounds R; tree depth; regularisation weights
      Initialise: Model parameters \theta_{PV}; best validation loss \mathcal{L}_{best} \leftarrow \infty
      for round r=1 to R do
             Sample minibatch \left\{\left(\mathbf{x}_{b}^{\text{PV}}(t), P_{\text{PV},b}(t+\tau)\right)\right\}_{(t,b)\sim\mathcal{M}}
 5:
             Predict: \hat{P}_{PV,b}(t+\tau) = XGBoost_{\theta_{PV}}(\mathbf{x}_b^{PV}(t))
6:
             Compute training loss \mathcal{L}(P_{PV}, \hat{P}_{PV}) using Eq. (9)
7:
             Update \theta_{PV} \leftarrow \theta_{PV} - \ell_{PV} \cdot \nabla_{\theta_{PV}} \mathcal{L}(P_{PV}, \hat{P}_{PV})
             Evaluate on validation set:
9.
                      \mathcal{L}_{val} \leftarrow ValidationLoss(\theta_{PV})
10:
              if \mathcal{L}_{val} < \mathcal{L}_{best} then
                     Save current model; \mathcal{L}_{best} \leftarrow \mathcal{L}_{val}
13:
              if early stopping condition met then
                    break
              end if
16: end for
17: Output: Trained model XGBoost<sub>\theta_{PV}</sub>, mapping \mathbf{x}_{b}^{PV}(t) to forecast \hat{P}_{PV,b}(t+\tau)
```

Algorithm 2 describes the XGBoost training process for PV forecasting. The model learns from feature-target pairs based on historical irradiance, temperature, and temporal variables. Each boosting round fits a regression tree to the residuals, iteratively updating parameters $\theta_{\rm PV}$ to minimise the regularised loss in Eq. (9). Validation loss is monitored to enable early stopping, and the final model is selected based on the lowest error. The trained model maps inputs $\mathbf{x}_{\rm PV}^{\rm PV}(t)$ to forecasts $\hat{P}_{\rm PV}$, b for each PV-enabled bus $b \in \mathcal{B}_{\rm PV}$.

III. FORECAST-AWARE CONTROL WITH GAN-BASED SCENARIO GENERATION

To model the stochastic variability of future power profiles, separate GANs are trained for EV demand and PV generation. Each GAN consists of a generator $\mathcal{G}_{\theta}^{(\cdot)}$ and a discriminator $\mathcal{D}_{\phi}^{(\cdot)}$, where $(\cdot) \in \{\text{EV}, \text{PV}\}$ indicates the domain. The generator maps a latent input $\mathbf{z} \sim p(\mathbf{z})$ (e.g., a multivariate Gaussian) to a synthetic spatiotemporal trajectory:

$$\tilde{\mathcal{P}}^{(\cdot)} = \mathcal{G}_0^{(\cdot)}(\mathbf{z}) \in \mathbb{R}^{|\mathcal{T}| \times |\mathcal{B}|},\tag{10}$$

where $\tilde{\mathcal{P}}^{(\cdot)}$ represents the generated EV or PV power profile across time \mathcal{T} and network buses \mathcal{B} .

The discriminator is trained to distinguish real from generated samples, and both networks are optimised via the standard adversarial loss [10]:

$$\min_{\boldsymbol{\theta}^{(\cdot)}} \max_{\boldsymbol{\phi}^{(\cdot)}} \left[\mathbb{E}_{\mathcal{P}^{(\cdot)} \sim p_{\text{data}}} [\log \mathcal{D}_{\boldsymbol{\phi}}^{(\cdot)}(\mathcal{P}^{(\cdot)})] + \mathbb{E}_{\mathbf{z} \sim p(\mathbf{z})} [\log (1 - \mathcal{D}_{\boldsymbol{\phi}}^{(\cdot)}(\mathcal{G}_{\boldsymbol{\theta}}^{(\cdot)}(\mathbf{z})))] \right]$$
(11)

Once trained, the generator produces multiple forecast trajectories $\{\tilde{\mathcal{P}}^{(\kappa)}\}_{\kappa=1}^{\mathcal{K}}$, each representing a plausible realisation of future EV or PV power. These trajectories serve as input scenarios for a stochastic control optimisation, enabling robust decision-making under uncertainty.

Let $\{u(t)\}_{t\in\mathcal{T}}$ denote the sequence of control decisions (e.g., EV charging rates and ESS dispatch). For each scenario $\kappa=1,\ldots,\mathcal{K}$, let $\tilde{P}_{\mathrm{EV},b}^{(\kappa)}(t)$ and $\tilde{P}_{\mathrm{PV},b}^{(\kappa)}(t)$ be the forecasted EV load and PV output at bus b, respectively. We define:

$$\tilde{P}_{\text{EV}}^{(\kappa)}(t) = \{\tilde{P}_{\text{EV},b}^{(\kappa)}(t)\}_{b \in \mathcal{B}}, \quad \tilde{P}_{\text{PV}}^{(\kappa)}(t) = \{\tilde{P}_{\text{PV},b}^{(\kappa)}(t)\}_{b \in \mathcal{B}}. \tag{12}$$

The objective is to minimise the expected cost across all scenarios, combining energy supply costs (net of PV generation) with penalties for unmet EV charging demand:

$$\min_{\{u(t)\}} \frac{1}{\mathcal{K}} \sum_{\kappa=1}^{\mathcal{K}} \sum_{t \in \mathcal{T}} \left[\lambda_1 \cdot \underbrace{\sum_{b \in \mathcal{B}} c_b(t) \cdot \left(u_b(t) - \tilde{P}_{\text{PV},b}^{(\kappa)}(t) \right)}_{\text{net energy cost}} + \lambda_2 \cdot \underbrace{\sum_{b \in \mathcal{B}} \max \left\{ 0, \ \tilde{P}_{\text{EV},b}^{(\kappa)}(t) - u_b(t) \right\}}_{\text{unmet EV demand penalty}} \right]$$
(13)

where $u_b(t)$ is the control action at bus b, and $c_b(t)$ is the local energy cost. The λ_1 and λ_2 are weighting coefficients.

All control decisions u(t) must satisfy a few constraints across network elements. Firstly, each bus $b \in \mathcal{B}$ is subject to local device capacity limits as $0 \le u_b(t) \le P_{\mathrm{EV,max}}^{(b)} + P_{\mathrm{ESS,max}}^{(b)}$, where $u_b(t)$ denotes the combined control action (e.g., EV charging plus ESS dispatch), and $P_{\mathrm{EV,max}}^{(b)}$, $P_{\mathrm{ESS,max}}^{(b)}$ are the respective rated capacities at bus b.

Secondly, the energy state of each storage unit $s \in \mathcal{S}$, whether stationary or mobile, evolves according to:

$$SoC_s(t+1) = SoC_s(t) + \eta \cdot P_s^{charge}(t) \cdot \Delta t - \frac{1}{n} \cdot P_s^{discharge}(t) \cdot \Delta t,$$
 (14)

subject to the operational bounds $SoC_{min} \leq SoC_s(t) \leq SoC_{max}$, where $\eta \in (0,1]$ is the round-trip efficiency and Δt is the time step duration (in hours). It should be noted that Eq. (14) assumes a simplified linear charging/discharging model with constant round-trip efficiency η , which does not account for practical constraints such as dynamic charging profiles (e.g., constant-current or constant-voltage), charger power limitations, temperature effects, or battery degradation.

Thirdly, PV generation is constrained by both inverter limits and environmental availability:

$$0 \le P_{\text{PV},b}(t) \le \min\left(P_{\text{PV},\text{max}}^{(b)}, f_{\text{irr}}(t) \cdot A_b \cdot \eta_{\text{PV}}\right), \tag{15}$$

where A_b is the PV panel area and η_{PV} is the power conversion efficiency.

Finally, the forecasting and optimisation models operate on a short-term horizon $\tau \in \{1, 2, \dots, H\}$ to support real-time operational tasks such as scheduling and energy dispatch.

The complete control procedure is summarised in Algorithm 3. The optimisation is formulated as a linear programme with a linear objective and piecewise-linear penalties represented via auxiliary slack variables. All operational constraints are linear. To enhance tractability, binary constraints (e.g., charging/discharging exclusivity) are relaxed, allowing continuous control within [0,1], which accelerates solution time at the expense of some modelling precision. A rolling-horizon strategy is employed: at each timestep, new GAN-based forecasts $\{\tilde{P}_{\rm EV}^{(\kappa)},\tilde{P}_{\rm PV}^{(\kappa)}\}$ are generated, the linear programme is solved, the first control action u(t) is applied, and the process repeats to adapt to real-time conditions.

IV. CASE STUDY AND RESULTS

The proposed framework is validated on the IEEE 33bus distribution system using data from MATPOWER. Static EVCSs are located at Buses 9, 17, and 32 with rated loads of

Algorithm 3 Scenario-based rolling optimisation under forecast uncertainty

```
1: Input: Trained GAN generators \mathcal{G}_{\theta}^{\text{EV}}, \mathcal{G}_{\theta}^{\text{PV}}, H, \mathcal{K}, \lambda_1, \lambda_2, \{c_b(t)\}
     for each time step t \in \mathcal{T} do
            Generate scenarios:
            for \kappa = 1 to K do
                  Sample latent vector \mathbf{z}^{(\kappa)} \sim p(\mathbf{z})
\tilde{P}_{\text{EV}}^{(\kappa)}(t:t+H) \leftarrow \mathcal{G}_{\theta}^{\text{EV}}(\mathbf{z}^{(\kappa)}), \quad \tilde{P}_{\text{PV}}^{(\kappa)}(t:t+H) \leftarrow \mathcal{G}_{\theta}^{\text{PV}}(\mathbf{z}^{(\kappa)})
5:
6:
7:
            end for
8:
            Solve optimisation:
            Compute control sequence \{u(t), \ldots, u(t+H)\} by solving linear programme
      using all K scenarios
             Implement control: Apply first-step decision u(t)
11: end for
12: Output: Control trajectory \{u(t)\}_{t\in\mathcal{T}}
```

30 kW, 50 kW, and 60 kW, respectively. Dynamic EV demand is synthesised using the NREL commercial fleet dataset and VISTA travel data, generating 100 mobile EV agents randomly assigned across Buses 2-33 based on stochastic availability [13], [14]. Stationary storage systems are installed at Buses 7, 19, and 29 with capacities between 30-40 kWh and peak power support of 200 kW during 17:00-21:00. PV systems are installed at Buses 5, 11, and 24 with 40 kW inverters.

A. Forecasting accuracy evaluation

Short-term forecasts of EV charging demand and PV generation are evaluated over a 24-hour horizon. Fig. 1 presents forecasting results for representative EV and PV buses (9, 17, and 32 for EV; 5, 11, and 24 for PV). Fig. 1a compares actual and predicted EV charging profiles using LSTM and ConvLSTM models. The selected buses exhibit different temporal profiles: Bus 9 shows a pronounced evening peak, Bus 17 a delayed morning ramp, and Bus 32 minimal demand variation. ConvLSTM consistently outperforms LSTM, particularly under high-variability conditions, owing to its ability to capture spatiotemporal patterns across distributed EVCS nodes. Table I summarises the one-hour-ahead MAE for each method. For example, at Bus 9, ConvLSTM reduces the MAE from 1.62 kW (LSTM) to 1.28 kW, with similar improvements across other EV buses. For PV forecasting, XGBoost achieves high accuracy, with MAE values consistently below 0.25 kW across all evaluated nodes. Fig. 1b shows the distribution of PV forecast residuals at Buses 5, 11, and 24. The tight interquartile ranges and lack of significant outliers confirm the robustness of the XGBoost model under stable weather conditions. Forecast performance is further evaluated across multiple prediction horizons $\tau \in \{1, 2, 3, 4\}$ using normalised root mean square error (NRMSE) as a scale-independent metric. Fig. 1c shows that forecast error increases with horizon length due to growing uncertainty. EV buses with higher volatility (e.g., Bus 9) exhibit the steepest increase in NRMSE, while smoother profiles (e.g., Bus 32 and PV buses) maintain relatively low errors even at 4-hour horizons.

B. GAN scenario generation and validation

To evaluate the realism and statistical validity of the GANgenerated scenarios, key properties of synthetic EV charging demand profiles are compared against real data. Validation focuses on static EVCS nodes (Buses 9, 17, and 32), which serve

TABLE I. ONE-HOUR-AHEAD MAE (KW) ACROSS REPRESENTATIVE BUSES

Bus	LSTM	ConvLSTM	XGBoost (PV)
Bus 9 (EV)	1.62	1.28	_
Bus 17 (EV)	1.15	0.94	_
Bus 32 (EV)	0.88	0.79	_
Bus 5 (PV)	-	_	0.23
Bus 11 (PV)	-	_	0.21
Bus 24 (PV)	_	-	0.19

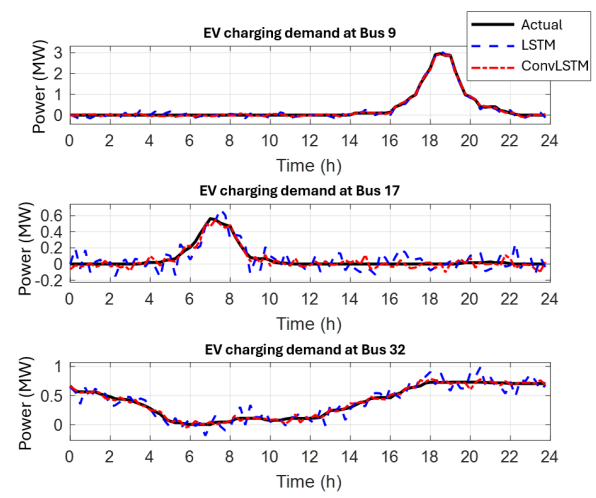
as control points for scheduling. As shown in Fig. 2, the time-varying mean and variance (capturing behavioural diversity and temporal uncertainty across scenarios) of GAN-generated trajectories closely match those of the real data. Notably, the evening peak around 18:00 is accurately reproduced in both magnitude and variability.

C. Scenario-based control performance

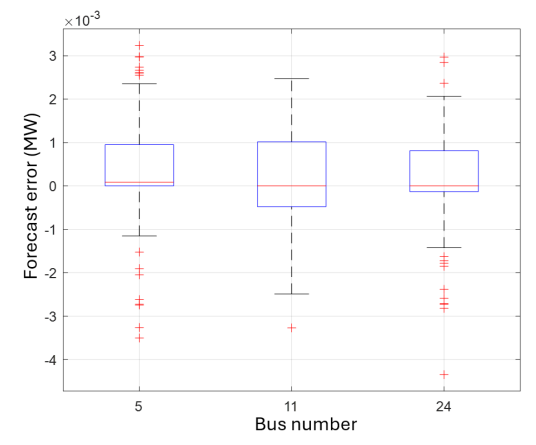
The scenario-based optimisation problem is implemented in MATLAB using the linprog solver from the Optimisation Toolbox. Fig. 3a illustrates the control trajectories at three representative buses under both scenario-based and deterministic strategies. The red solid line denotes the average control action across multiple forecast scenarios, while the shaded region represents the 90% confidence interval (CI), reflecting the variability of responses to forecast uncertainty. The blue dashed line corresponds to the deterministic control based on a single-point forecast. Compared to the deterministic baseline, the scenario-based strategy dynamically adjusts both the timing and magnitude of actions to account for uncertainty, particularly at Buses 17 and 32, which experience higher temporal variability in EV demand. Fig. 3b evaluates the impact of the number of forecast scenarios \mathcal{K} on control performance. As K increases, both average energy cost and unmet demand decrease due to improved uncertainty representation. However, performance gains plateau beyond K = 15, indicating a practical trade-off between accuracy and computational cost. Fig. 3c presents a contour plot of the total objective cost as a function of the weighting parameters λ_1 (energy cost) and λ_2 (unmet demand penalty) in Eq. (13). A clear trade-off is observed: increasing λ_1 favours cost minimisation, while higher λ_2 emphasises demand satisfaction. The optimal tradeoff occurs near $\lambda_1 = 2$, $\lambda_2 = 3$.

V. CONCLUSIONS

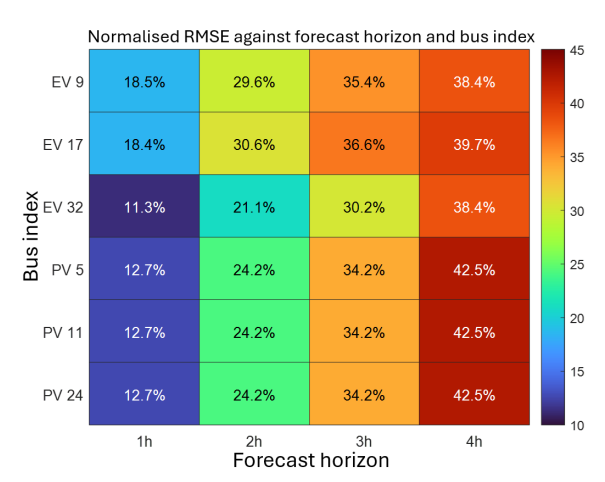
This paper proposed a dual-stage, AI-driven framework for resilient energy management in distribution networks with high EV and PV penetration. The approach combines short-term forecasting, via LSTM/ConvLSTM for EV demand and XGBoost for PV generation, with GAN-based scenario generation to support robust, uncertainty-aware control. Case studies on the IEEE 33-bus system demonstrate improved forecasting accuracy, realistic scenario generation, and enhanced control adaptability under uncertainty. ConvLSTM effectively captures spatiotemporal EV patterns, while XGBoost provides reliable PV predictions. GANs enable scenario-based strategies that outperform deterministic baselines, especially under volatile



(a) EV charging forecasts using LSTM and ConvLSTM models at three buses with distinct demand patterns (Bus 9: peak, Bus 17: delayed, Bus 32: minimal).



(b) Distribution of PV forecast residuals using the XGBoost model across PV buses.



(c) Normalised RMSE (%) for EV charging and PV generation forecasts across multiple prediction horizons.

Fig. 1. Forecasting accuracy evaluation for EV and PV models.

conditions. A trade-off between energy cost and demand satisfaction was observed, emphasising the need for balanced

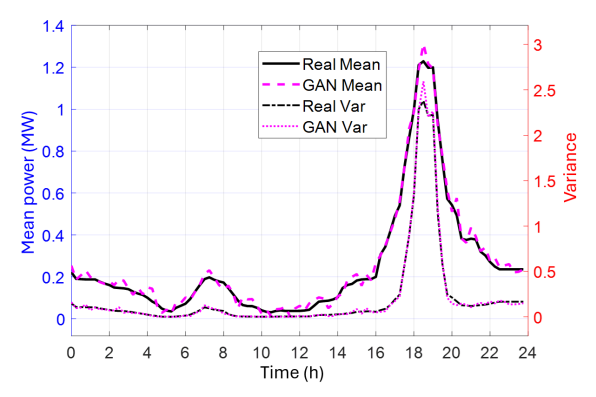


Fig. 2. Comparison of time-varying mean and variance between real and GAN-generated EV demand samples at EVCS buses (9, 17, 32).

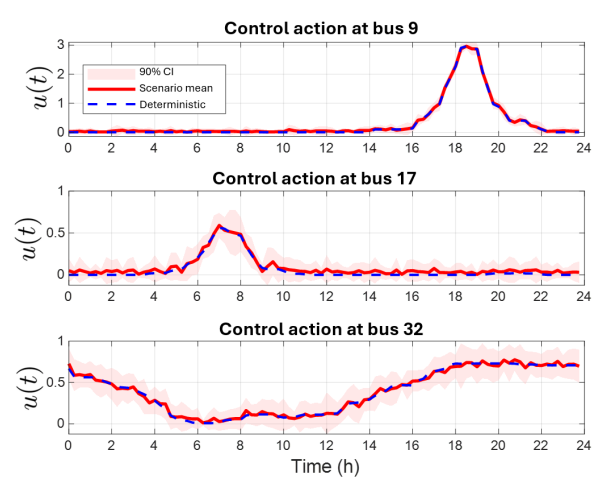
parameter tuning. While the framework shows strong performance, practical deployment requires addressing training costs, data infrastructure, and real-time integration. Future work will explore lightweight models, online adaptation, and integration with distribution automation systems.

ACKNOWLEDGMENT

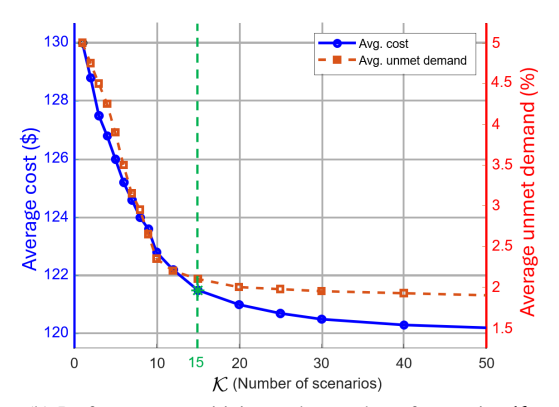
The work is supported by the U.K. Leverhulme Trust grant RPG-2023-107.

REFERENCES

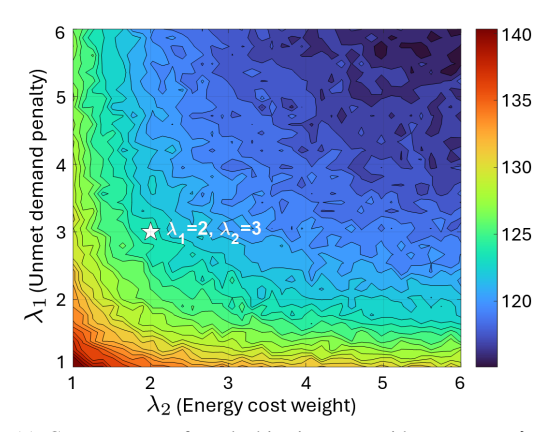
- [1] F. N. Esfahani, J. Ebrahimi, A. Bakhshai, X. Ma and A. Darwish, "A Modular Bidirectional Topology for Grid-Tied PV Powered EV Chargers with Isolated Single-Stage Sub-Modules," *IECON 2024 - 50th Annual Conference of the IEEE Industrial Electronics Society*, Chicago, IL, USA, 2024, pp. 1-6.
- [2] F. Nasr Esfahani, A. Darwish, S. Alotaibi and F. Campean, "Hierarchical Control Design of a Modular Integrated OBC for Dual-Motor Electric Vehicle Applications," *IEEE Access*, vol. 12, pp. 196306-196327, 2024.
 [3] F. Nasr Esfahani, A. Darwish, and A. Massoud, "Loop-Shaping Control
- [3] F. Nasr Esfahani, A. Darwish, and A. Massoud, "Loop-Shaping Control Design for a New Modular Integrated On-Board EV Charger with RHP Zero Compensation," *IET Power Electron.*, vol. 18, 2025.
- [4] F. Mohammad, D. -K. Kang, M. A. Ahmed and Y. -C. Kim, "Energy Demand Load Forecasting for Electric Vehicle Charging Stations Network Based on ConvLSTM and BiConvLSTM Architectures," *IEEE Access*, vol. 11, pp. 67350-67369, 2023.
- [5] C. Qin, A. K. Srivastava, A. Y. Saber, D. Matthews and K. Davies, "Geometric Deep-Learning-Based Spatiotemporal Forecasting for Inverter-Based Solar Power," *IEEE Syst. J.*, vol. 17, no. 3, pp. 3425-3435, 2023.
- Based Solar Power," *IEEE Syst. J.*, vol. 17, no. 3, pp. 3425-3435, 2023.
 Y. Chai, L. Guo, C. Wang, Z. Zhao, X. Du and J. Pan, "Network Partition and Voltage Coordination Control for Distribution Networks With High Penetration of Distributed PV Units," *IEEE Trans. Power Syst.*, vol. 33, no. 3, pp. 3396-3407, May 2018.
- [7] M. I. El-Afifi, A. A. Eladl, B. E. Sedhom and M. A. Hassan, "Enhancing EV Charging Station Integration: A Hybrid ARIMA-LSTM Forecasting and Optimization Framework," *IEEE Trans. Ind. Appl.*, vol. 61, no. 3, pp. 4924-4935, May-June 2025.
- [8] F. Nasr Esfahani, N. Suri and X. Ma, "A Two-Level Machine Learning Framework for Managing EV Charging and Renewable Energy Curtailment in Smart Grids," ICCEP 2025 - 9th International Conference on Clean Electrical Power, Sardinia, Italy, 2025, pp. 1–6.
- [9] T. Xu et al., "SeqESR-GAN-Based Sparse Data Augmentation for Distribution Networks," *IEEE Trans. Industr. Inform.*, vol. 20, no. 11, pp. 12913-12923, Nov. 2024.
- [10] S. S. K. Madahi, A. S. Kamrani and H. Nafisi, "Overarching Sustainable Energy Management of PV Integrated EV Parking Lots in Reconfigurable Microgrids Using Generative Adversarial Networks," *IEEE Trans. Intell. Transp. Syst.*, vol. 23, no. 10, pp. 19258-19271, Oct. 2022.
- [11] P. Kumar Mohanty, K. Hemant Kumar Reddy, S. K. Panigrahy and D. Sinha Roy, "Leveraging Generative and Explainable AI for Electric Vehicle Energy Toward Sustainable, Consumer-Centric Transportation," *IEEE Access*, vol. 12, pp. 143721-143732, 2024.



(a) Scenario-based vs. deterministic control (in MW) at Buses 9, 17, and 32.



(b) Performance sensitivity to the number of scenarios K.



(c) Contour map of total objective cost with respect to λ_1 and λ_2 .

Fig. 3. Scenario-based control performance analysis.

- [12] W. Liu, H. Zhu and H. Yuan, "Uncertainty-Guided Optimal Scheduling of Automated Energy Internet," *IEEE Trans. Industr. Inform.*, vol. 18, no. 8, pp. 5662-5669, Aug. 2022.
- [13] National Renewable Energy Laboratory. (2021). Fleet Depot Charging Profiles Dataset. NREL Data Catalogue., [Online]. Available: https://data.nrel.gov/submissions/162. Accessed: Nov 10, 2024.
- [14] Y. Wu, S. M. Aziz, M. H. Haque, "Travel Datasets for Analysing The Electric Vehicle Charging Demand in a University Campus," *Data in Brief*, Vol. 54, p. 110335, 2024.